lubricants

MDPI

Review

Two-Dimensional Nanomaterials in Hydrogels and Their Potential Bio-Applications

Zhongnan Wang [1], Hui Guo [1], Ji Zhang [2], Yi Qian [1,3] and Yanfei Liu [4,*]

[1] School of Mechanical, Electronic and Control Engineering, Beijing Jiaotong University, Beijing 100044, China; zhn.wang@bjtu.edu.cn (Z.W.); 21121292@bjtu.edu.cn (H.G.); laird.qian@zimmerbiomet.com (Y.Q.)
[2] Beijing Jishuitan Hospital, Capital Medical University, Beijing 100035, China; drzhangji@126.com
[3] Beijing Montagne Medical Device Co., Ltd., Beijing 100176, China
[4] School of Mechanical Engineering, Beijing Institute of Technology, Beijing 100081, China
* Correspondence: liuyanfei@bit.edu.cn

Abstract: Hydrogels with high hydrophilicity and excellent biocompatibility have been considered as potential candidates for various applications, including biomimetics, sensors and wearable devices. However, their high water content will lead to poor load-bearing and high friction. Currently, two-dimensional (2D) materials have been widely investigated as promising nanofillers to improve the mechanical and lubrication performances of hydrogels because of their unique physical–chemical properties. On one hand, 2D materials can participate in the cross-linking of hydrogels, leading to enhanced load-bearing capacity and fatigue resistance, etc.; on the other hand, using 2D materials as nanofillers also brings unique biomedical properties. The combination of hydrogels and 2D materials shows bright prospects for bioapplications. This review focusses on the recent development of high-strength and low-friction hydrogels with the addition of 2D nanomaterials. Functional properties and the underlying mechanisms of 2D nanomaterials are firstly overviewed. Subsequently, the mechanical and friction properties of hydrogels with 2D nanomaterials including graphene oxide, black phosphorus, MXenes, boron nitride, and others are summarized in detail. Finally, the current challenges and potential applications of using 2D nanomaterials in hydrogel, as well as future research, are also discussed.

Keywords: hydrogel; 2D nanomaterial; mechanical strength; lubrication behavior; nanofiller

Citation: Wang, Z.; Guo, H.; Zhang, J.; Qian, Y.; Liu, Y. Two-Dimensional Nanomaterials in Hydrogels and Their Potential Bio-Applications. *Lubricants* **2024**, *12*, 149. https://doi.org/10.3390/lubricants12050149

Received: 15 February 2024
Revised: 19 April 2024
Accepted: 25 April 2024
Published: 27 April 2024

1. Introduction

Hydrogels have attracted lots of attention for various applications, such as medical devices and micro-electrochemical systems (MEMS), because of their solid–liquid biphasic structures [1–4]. However, common polymer hydrogels such as polyvinyl alcohol (PVA), polyethylene glycol (PEG) and polyacrylic acid (PAA) have low mechanical strength (approximately 0.2 MPa~3 MPa), and poor antifouling and antibacterial ability [5–7]. Zwitterionic materials contain both cationic and anionic groups, with the overall charge being neutral. Zwitterionic hydrogels, like polymethylacrylamide sulfonate betaine (PSBMA), have a three-dimensional polymer network rich in cation and anion groups, and are electrically neutral at the macro level. They have a high water content and good resistance to bacterial adhesion, but their compressive strength (0.08 MPa) and lubricating ability ($\mu \approx 0.03$) are still insufficient [8]. Human cartilage with a complex lubrication mechanism exhibits a super-low sliding friction coefficient (below 0.01) and compressive strength (around 18 MPa). Therefore, there is still a significant gap in the mechanical and lubricating properties between traditional hydrogels and natural cartilage. Introducing nanofillers into hydrogels is an effective strategy to improve the mechanical and lubrication properties.

Two-dimensional (2D) nanomaterials are connected by strong covalent or ionic bonds within the layers and weak van der Waals forces between the layers [9,10]. Recently, 2D nanomaterials have been systematically investigated in the fields of bionics and wearable

medical devices because of their unique layered structures, physicochemical characteristics and good biocompatibility [11,12]. Moreover, graphene and MXene materials also exhibit extremely high mechanical strength [13,14]. Also, MXene and graphene oxide (GO) can offer reduced friction and wear of counterparts [15]. Subsequently, some studies on new classes of 2D nanomaterials with unique properties have been reported. Black phosphorus (BP) and hexagonal boron nitride (h-BN), used as typical 2D nanomaterials, show also excellent performance in terms of strength improvement and friction reduction [16–19]. When BP nanosheets are deposited on the silicon nitride (Si_3N_4) surface, the shear action of the contact interface promotes the formation of phosphorus oxide with low shear on the BP surface, leading to a stable sliding friction coefficient of 0.001 in a pure water environment [20]. As a lubricating additive, 2D nanomaterials including GO, BP, MXene and h-BN will form a tribochemical or physical adsorption layer at the solid–liquid interface, which enhances the anti-friction and anti-wear properties.

Various 2D nanomaterials (Figure 1) exhibit different functionalized properties for medical applications, such as use in biosensors, cartilage repair, skin tissue engineering and bone reconstruction [21]. Marian et al. [22] reviewed the unique structural properties of 2D materials, including their large surface to volume ratio, adjustable surface chemistry, inherent biocompatibility, antibacterial/antiviral activity, and non-cytotoxicity, which show great potential for biomedical applications, such as load-bearing implants, dental implants, bone fracture fixation, invasive surgical devices, cardiovascular devices, contact lenses, and bio-MEMS/NEMS. Two-dimensional materials can be used as protective coatings, fillers for composite materials, or additives for fluid mixtures, allowing for the effective adjustment and control of biotribological behavior. Specifically, GO might be used as a reinforcement of artificial cartilage, while BP has the potential to promote bone growth. The unique properties of 2D materials make them promising nanofillers for use in hydrogels to improve the mechanical and tribological performances in bioengineering applications.

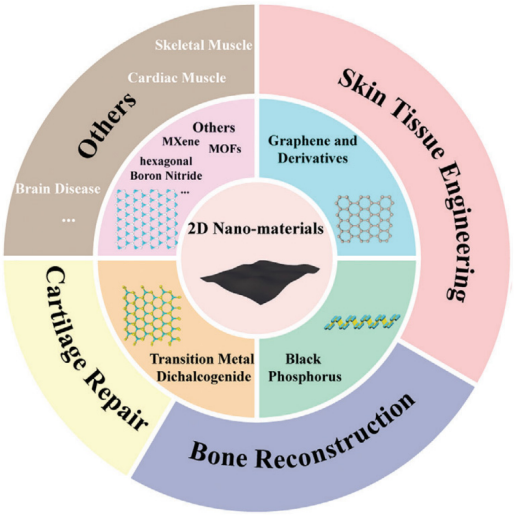

Figure 1. Various types and potential applications of 2D nanomaterials used in tissue engineering [21], copyright (2021), with permission from Wiley.

The introduction of GO at the nanoscale can significantly improve the mechanical and tribological properties of zwitterionic hydrogels, indicating their great potential for numerous applications [23]. Also, the combination of hydrogels and other 2D materials has yielded high-performance bioelectronic devices, which has promoted the development of biosensors and bioelectronics. However, 2D nanomaterials still have some inherent shortages, such as low synthesis efficiency and high economic cost, restricting their actual bioapplications. Moreover, the excellent mechanical and tribological behaviors of 2D nanomaterials with a feasible functional design mean they are often used as potential nano-additives for different load-bearing and lubrication systems. As a functional additive,

the dispersion of 2D nanomaterials in hydrogels affects their interaction with polymer molecular chains, thus reducing the homogeneity of the overall network structure.

Within this work, the authors review the most recent research achievements of typical 2D materials used as nanofillers of hydrogel. Moreover, the fundamental mechanisms and functional properties of these 2D materials used as nanofillers of hydrogel are reviewed in detail. In addition, the unsolved issues and optimistic outlooks are also discussed. This review aims to provide useful insights and guidelines related to the design and development of hydrogels for various biomedical applications, and facilitate a continuously updated understanding of the influence of the typical 2D nanomaterials on mechanical and tribological performances.

2. Mechanical and Friction Properties of Hydrogels with 2D Nanomaterials

In 2004, Geim and Novoselov [24] obtained graphene via tape stripping; this material has excellent electron transport properties and electrical conductivity at room temperature. Graphene has excellent electronic properties, an extremely high specific surface area, and great potential applicability in the field of optoelectronics and catalytic reactions. h-BN, BP, MXene, and transition metal sulfides (TMDs) have graphene-like structures, which are stacked into massive crystals of different structures by van der Waals force. They show excellent optical, electrical, and chemical stability on a macro level, enriching the properties of 2D materials and promoting their applications as functional nano-additives. Table 1 gives the key properties of typical 2D materials.

Table 1. Mechanical properties of hydrogels reinforced by two-dimensional nanomaterials.

Nanoparticles	Elastic Modulus (GPa)	Tensile Strength (GPa)	Elastic Strain
GO	207.6 ± 23.4 [25]		0.4% [26]
BN	865 ± 73 [25]	70.5 ± 5.5 [27]	2.5 ± 3.0% [27]
BP	19.5~41.3 [28]	4.09~8.42 [29]	0.48% [28]
$Ti_3C_2T_x$ [13]	483.5 ± 13.2	15.4 ± 1.92	3.2%

2.1. Graphene Oxide

GO has more oxygen-containing functional groups, and can more easily physically react with other substances to yield the various characteristics of polymers, colloids or amphoteric molecules. GO has a special physically layered structure and stable chemical properties, and it can fill in the scratches and wear pores on friction surfaces, repair the damaged surfaces of friction pairs, enhance the anti-wear ability of concave and convex contacting interfaces, and lower the friction coefficient of material surfaces. Therefore, GO can be used as a nanofiller to enhance the lubrication and anti-wear properties of polymer hydrogels for a wide range of applications [23,30,31]. The interlayer structure and the number of functional groups in GO affect the shear resistance of the interface [32]. GO nanosheets have been annealed at different temperatures to obtain h-GO with different numbers of hydroxyl functional groups. It is proven that the number of oxygen-containing functional groups and the interlamellar distance will limit the hydrogen bonding of the molecules, and thus affect the lubrication ability of GO [33]. Moreover, the excellent lubrication performance of GO in metallic contact contexts means that the slip of the GO layer with low shear strength reduces the friction resistance at the interface, compared to a single physical deposition film [34].

The excellent biocompatibility of GO means it can also be used as a functional filler to enhance the properties of biological materials [35,36]. Hydrogel is a type of polymer material containing a hydrophilic three-dimensional network, which has a wide range of applications in biomedical research fields such as bionic skin, and bionic tissues and organs [37,38]. However, the traditional hydrogels lack sufficient mechanical and lubrication properties to completely meet the practical needs of bioapplications [39–41]. As a functional nanofiller, GO can be combined into a polyvinyl alcohol (PVA)/poly (N-isopropylacrylamide) (PNIPA) hydrogel to yield a good thermal response ability through

free radical cross-linking. The mechanical properties of GO-PVA/PNIPA hydrogels can be enhanced with an increase in GO mass fraction, which has a potential application in temperature sensor research [39]. The diversity of pore sizes within the hydrogel's architecture dramatically influences its mechanical attributes. As the content of graphene oxide (GO) increases to a threshold level, the pores transition from a microscale to a nanoscale uniform distribution, resulting in a more compact structure. It is this intricate porous morphology, characterized by interconnected pores at the nanoscale, that markedly enhances the hydrogel's mechanical robustness [39]. The composite hydrogel synthesized by adding GO to chitosan shows good shape memory and self-healing properties. The change of solution pH will affect the hydrogen bond and hydrophobic action of polymer chains, resulting in a change of the state of the cross-linked network and the pH response ability of the composite hydrogel [42,43]. In addition, the shape and structure of GO will also affect the dispersibility in solvent and the lubrication performance of the composite hydrogel [44]. Compared to other fillers (carbon fiber [45], metal nanoparticles [46], ceramics [47]), GO [48] shows excellent self-lubrication capabilities and mechanical strength. A polyacrylamide (PAAm) hydrogel was combined with GO to significantly reduce its friction coefficient and wear rate with supramolecular polyethylene [49] (Figure 2). By enhancing the layer spacing of GO with polyethylene glycol (PEG), hydroxyapatite (HA) particles can be uniformly distributed on the GO surface in order to obtain a GO-PEG-HA hybrid, which is added to the PVA polymer as a filler to prepare a PVA/GO-PEG-HA hydrogel with excellent biocompatibility. This nanocomposite hydrogel exhibited an enhanced compression strength (4.49 MPa) and a reduced sliding friction coefficient (0.06), compared with PVA hydrogel [50]. The introduction of GO into a PVA/polyacrylic acid (PAA)/polydopamine multifunctional coating could reduce the contact angle of the Ti6Al4V alloy surface and achieve better wettability, as well as improving the corrosion resistance and biocompatibility [51]. The improvement of the anti-corrosion efficiency of hydrogel coatings is attributed to the nucleophilic reaction between the epoxy and amino groups from GO and the active ions of SBF solution (Figure 3a). Also, the GO sheets at the interface of the PVA/PAA/GO/PDA hydrogel coating and a cortical bone sample might enable a significant reduction in friction coefficient (Figure 3b).

2.2. Boron Nitride

Recently, BN materials have attracted widespread attention from researchers as an outstanding filler to enhance the mechanical strength and lubrication of various functional hydrogels, due to their unique ultimate thermal stability, chemical inertness, and resistance to oxidation.

BN has a graphite-like lamellar structure and is thought to facilitate cartilage movement, just like in bearing systems [52]. Many studies suggest its promising potential use in biomedical applications such as artificial cartilages, drug delivery, tissue engineering, biosensors and actuators [53].

Jing et al. [54] prepared a hydroxylated boron nitride nanosheet (OH-BNNS)/PVA interpenetrating hydrogel that exhibited controllable reinforcements in mechanical responses. Impressive 45% and 43% increases in compressive and tensile strengths, respectively, could be achieved when the addition of OH-BNNS is only 0.12 wt. % (Figure 4). The superior intrinsic properties of distributed OH-BNNS and strong hydrogen bonding interactions between the OH-BNNS and PVA chains collectively contribute to the efficient load transfer. Yang et al. [55] found that hexagonal boron nitride nanoplatelets (BNNPs) grafted with amino acid could be used as functional fillers for simultaneously enhancing the mechanical and self-healing properties of the PVA hydrogel composites. The incorporated fillers provided hydrogen-bonding interactions between -OH groups on the PVA chain and the -COOH groups originating from AA moieties to offer excellent tensile strength and healing efficiency.

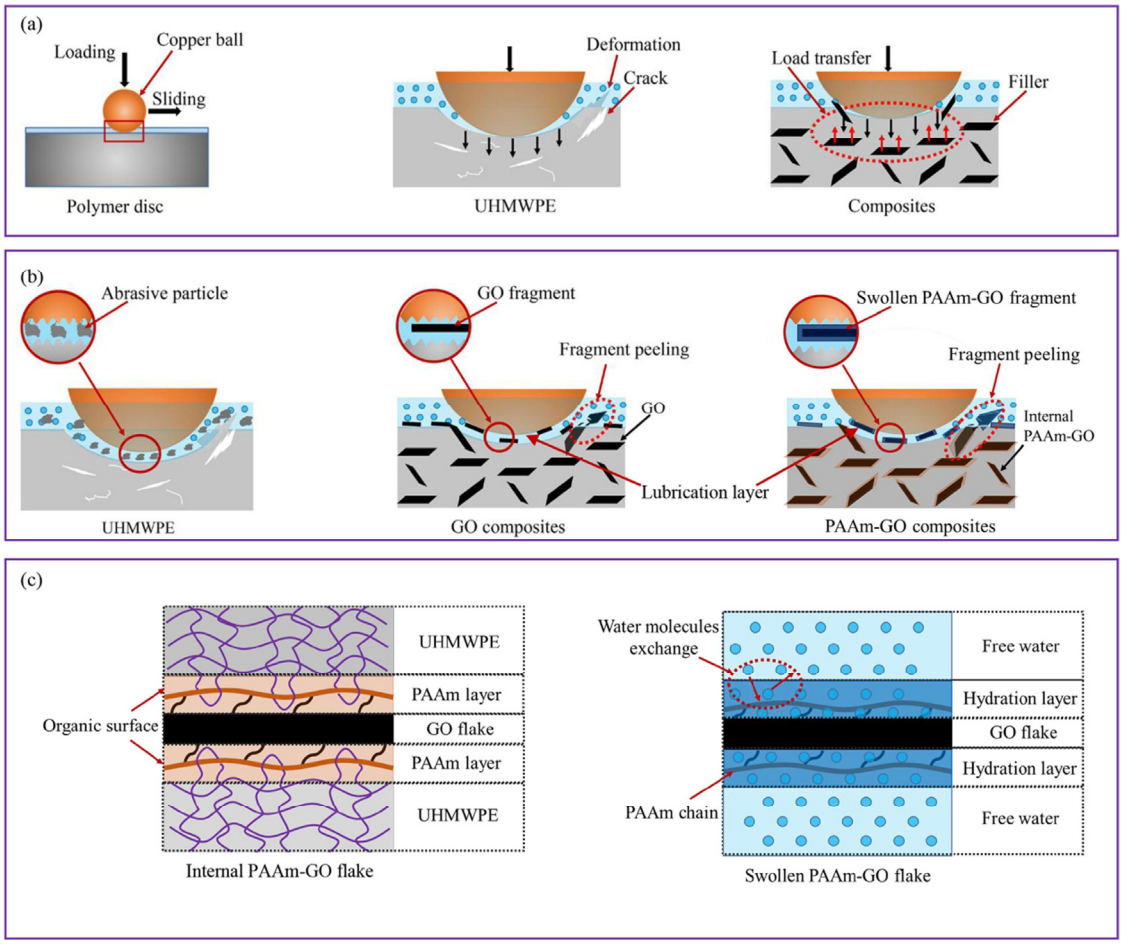

Figure 2. A comprehensive analysis of tribological mechanisms between GO and PAAm hydrogel. (**a**) The bearing statuses of UHMWPE and the composites; (**b**) the lubricating characteristics of the polymers; and (**c**) two states of PAAm-GO flakes [49], copyright (2021), with permission from Elsevier.

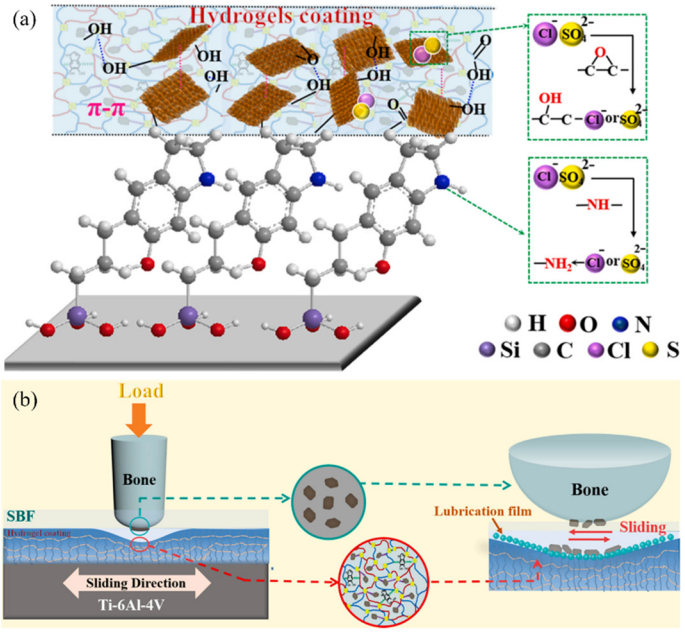

Figure 3. Schematic diagram of the mechanisms of GO-based hydrogel coating. (**a**) Anticorrosion mechanisms of PVA/PAA/GO/PDA samples; (**b**) biotribological mechanisms of PVA/PAA/GO/PDA samples [51], copyright (2023), with permission from Elsevier.

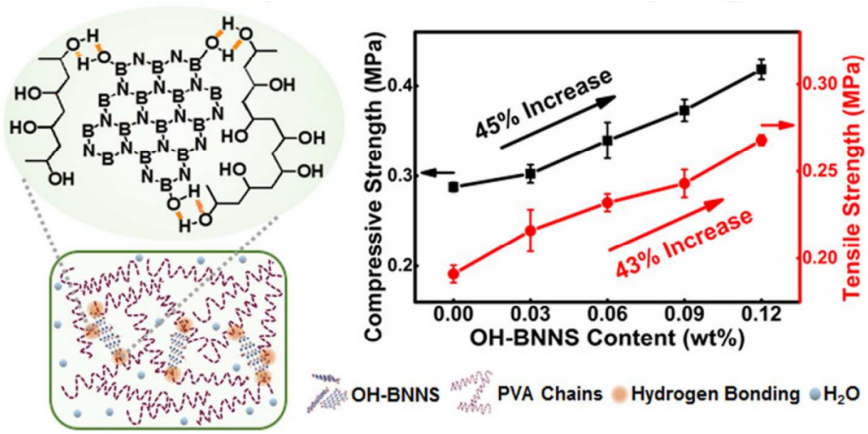

Figure 4. Structural characterization and mechanical responses of OH-BNNS/PVA composite hydrogels [54], copyright (2023), with permission from ACS.

Xue et al. [56] used surface-modified BN nanosheets as nanofillers to fabricate a novel PAA/BNNS-NH_2 composite hydrogel via hierarchical physical interactions. The addition of BNNS could enhance the mechanical properties of the PAA hydrogel, including offering a fracture stress of ~1311 kPa and toughness of ~4.7 MJ m^{-3}. Jiang et al. [57] also found that a dual crosslinked BNNS/PAA nanocomposite hydrogel could recover its mechanical strength even following severe structural breakdowns, such as after three consecutive cutting cycles. The functionalized material was prepared by Liu et al. [58] to effectively improve the mechanical modulus of polyurethane (PU) hydrogels from 1635 to 2776 kPa with only 0.066 wt. % BNNS loading, which could be highly useful in printed electronics. This enhancement can be primarily attributed to the robust hydrogen bonding interactions between OH-BNNS and the PU-based hydrogel matrix. Nevertheless, an excessive incorporation of OH-BNNS may lead to agglomeration and the introduction of more defects, which can compromise the material's integrity and facilitate stress concentration. Hu et al. [59] prepared ca-BNNS/PAAm nanocomposite hydrogels with high water retentivity and flexibility. They showed and elongation that exceeded 10,000% and a compressive strength of 8 MPa at 97% strain, and there was no obvious damage after the removal of the compression force. BNNSs, as a promising material, could provide excellent water retentivity and flexibility for the development of high-performance hydrogels.

A physically linked 3D f-BNNS/clay/PNIPAM ternary networks (TN) hydrogel was built by Tong et al. [60] using functionalized boron nitride nanosheets (f-BNNS) with H-grafted nitrogen/OH-grafted boron atoms. A soft polymer network embedded with 2D hard f-BNNS could improve the mechanical properties through effective load transfer and dissipated energy via the incorporation of a sacrificial non-covalent hydrogen bond. This high-toughness TN hydrogel might be used in various application fields, such as sensors, tissue engineering and flexible devices. Goncu et al. [61] found that the introduction of BN with different structures could play a dominant role in affecting the dynamic viscosity of the zero-shear point and the deformation rate, as well as the viscoelastic properties of the hybrid hydrogel. The lamellar structures of h-BN have been considered to be part of an effective method of joint injections for the treatment of osteoarthritis (OA).

2.3. Black Phosphorus

Black phosphorus (BP) is a graphite-like photoelectric material with an anisotropic lamellar structure and low interlayer interaction. Phosphorus atoms are deposited in a two-dimensional plane to form a folded honeycomb, which means it has great tensile and extrusion characteristics in the atomic plane, and it can be deformed under external forces to change its conductive ability [62]. BP's interlayer spacing (0.53 nm) is larger than that of GO (0.36 nm), which is conducive to the insertion and removal of ions, imparting broad application prospects in the fields of lithium-ion batteries and supercapacitors [63].

BP is prone to oxidation when exposed to air, forming phosphorus oxide with very low shear strength, which can achieve super-lubricity in a pure water environment [12]. The introduction of BP into carbon fiber (CF)/PTFE composites could help to form a lubrication film composed of phosphorus oxide and phosphoric acid at the contact interface, resulting in a reduced friction coefficient and the disappearance of adhesive wear [64,65]. Wu et al. [66] found that the formation of a highly mobile water layer on the oxidized BP/SiO_2 interface could impart a super-lubricity phenomenon, and the lubricious liquid water layer notably reduced the interfacial shear strength (~0.029 MPa).

However, single nanoparticles have been demonstrated to be insufficient when used as an additive to optimize the lubricating property of materials. By means of sol-gel, high-energy ball milling and mechanical stirring, BP could be combined with titanium dioxide (TiO_2) [67], silver nanoparticles [68], MoS_2 [69] or other nanoparticles, and used in oil-based lubricants [70] and water-based lubricants [71] to form a mixed lubrication additive. The synergistic effects of BP and the above particles further improved the anti-friction and anti-wear properties of friction materials. For example, BP powder was prepared by high-energy ball milling and then combined with TiO_2 to prepare BP/TiO_2 nanocomposites via a solvothermal reaction. The rolling tribology experiment (Figure 5) shows that the friction coefficient and wear rate of BP/TiO_2 nanocomposites are significantly lower than those of BP and TiO_2, which is due to the formation of a tribochemical reaction film on the surfaces of BP/TiO_2 nanocomposites, and the repair effects of TiO_2 on the worn area. The results show that the composite nanoparticles can repair the worn surface and form a complex tribochemical reaction film on the surface of the material, which contributes to the friction interface becoming smoother with the addition of nanoparticles, and the wear rate of the material surface being significantly reduced [69].

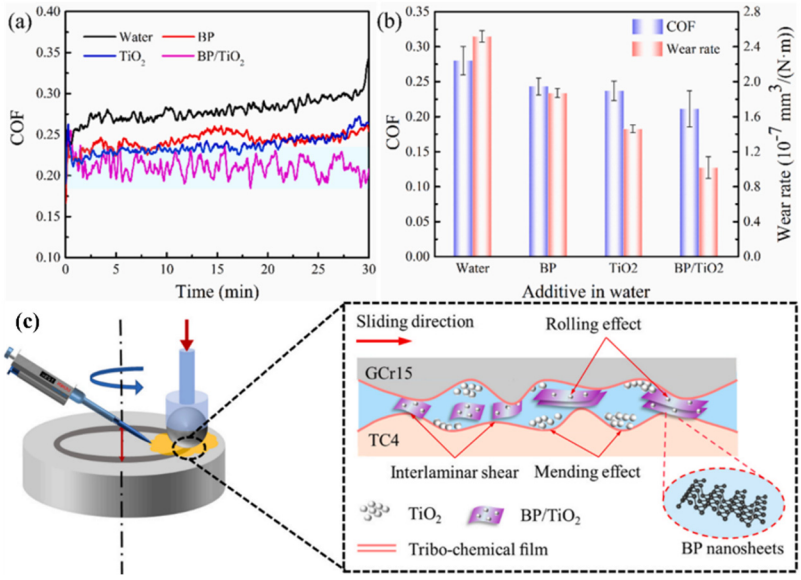

Figure 5. Friction experiments and synergy lubrication model of nanocomposite lubrication additives. (**a**) The curve of COFs and (**b**) wear rates of Ti–6Al–4V alloy discs of ultrapure water, BP water-based lubrication additive, TiO_2 lubrication additive, and BP/TiO_2 lubrication additive. (**c**) Collaborative lubrication mechanism of BP/TiO_2 composite nanoparticles [69], copyright (2022), with permission from Elsevier.

In addition, BP has excellent photothermal conversion efficiency and inherent photoacoustic properties, which endow it with potential applications in the biomedical field [72]. The encapsulated black phosphorus nanosheet (BPN) could be used to stably provide modest amounts of phosphorus for the enhancement of the compressive strength (up to 0.15 MPa) and compressive moduli (arrive at 0.9 MPa) of hydrogels. BPNs were successfully encapsulated within the hydrogel matrix to create a thicker structure with permeable holes.

This innovation results in a reinforced network architecture in the nanocomposite hydrogels. Additionally, the optimized porous configuration endows these hydrogels with enhanced water absorption capabilities, a feature that is particularly advantageous for facilitating the nutrient supply required for cellular growth and proliferation. Moreover, the phosphoric acid component contained in BP can promote the growth and reproduction of chondrocytes, which can be applied as bionic materials in the field of bone tissue engineering (Figure 6a) [73]. BP was mixed with chitosan (CS) for deposition on polyetheretherketone (PEEK) bone scaffold by 3D printing technology. Then, cell culturing in vitro and the growth of cells implanted into mice showed that this scaffold has good biological activity and can promote the expression of osteogenic genes [74]. The tests on the synthesized skeleton, including for its antibacterial property, in vitro osteosarcoma ablation, in vivo tumor ablation, in vitro cytocompatibility, in vitro osteogenic activity and in vivo bone regeneration, were performed to investigate its biocompatibility. Alkaline phosphatase was used as a marker of osteogenic differentiation to evaluate its capacity to promote bone growth. A novel scaffold system consisting of a 3D PEEK scaffold substrate and a BP/CS composite coating can effectively fill bone defects and provide the required mechanical support (Figure 6b).

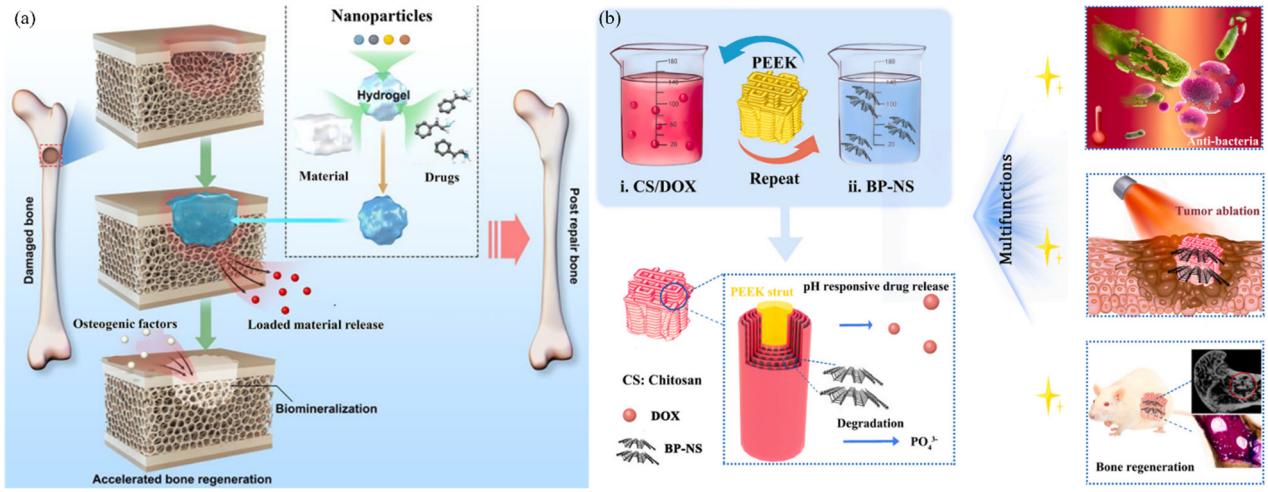

Figure 6. (**a**) Schematic illustration of BPN-containing hydrogel with the excellent mechanical behaviors required in bone tissue engineering [73], copyright (2022), with permission from Taylor & Francis. (**b**) Schematic of BP-NS/CS-DOX composite coating on a sulfonated PEEK scaffold with multiple functions [74], copyright (2022), with permission from Elsevier.

2.4. MXenes

In 2011, researchers from Drexel University obtained MXene materials by etching Al into ternary layered carbide Ti_3AlC_2 with hydrofluoric acid. These were composed of transition metal carbides, nitrides or carbon nitrides [75]. MXene has a two-dimensional graphene-like structure, excellent self-lubricating ability, and many groups on the surface, which means it has been the subject of much research in the fields of energy storage, catalysis, lubrication, and antibacterial and electromagnetic shielding [76]. Chhattal et al. [77] reviewed the effects of different synthesis methods on the properties of MXene (mechanics, lubrication and surface properties), and suggested that improving the synthesis of MXene 2D materials is an important way to effectively improve their properties. The tribological behavior of MXene at the micro and macro scales, as well as its research status as a coating, lubricating additive and composite reinforcing phase, is emphasized. It is considered that the dispersion and adsorption of MXene on the surface of the material greatly affects the lubrication effect of the contact area. The MXene interlayer has a weak force and is easy to peel off, leading to good self-lubricating properties. MXene is coated on the surface of stainless steel and silicon wafers to generate a dense $Ti_3C_2T_x$ friction film at the contact

interface, which significantly reduces the friction coefficient and wear rate of the sliding interface [78,79]. Compared with traditional carbon-based lubrication fillers (graphite, graphene, carbon nanotubes), MXene has strong interface coupling properties [80].

Combining low-dimensional nanostructured materials with MXene can improve its dispersion performance. Das et al. [81] summarized the mechanical, magnetic and thermal stability and photoelectrical properties of composite nanomaterials synthesized from MXene and low-dimensional nanomaterials (quantum dot, magnetic nanoparticles, nonmagnetic metal oxides and precious metals), as well as the application status of composite nanomaterials in the fields of sensors, new energy storage, catalysts, etc. MXene is mixed with metal nanoparticles and MoS_2 as a lubrication additive to enhance the mechanical strength of the physical adsorption film on the friction surface of the MXene layer, which imparts outstanding lubrication and anti-wear properties under high stress, and further provides a theoretical basis for the development of multi-functional lubrication materials [82,83]. The Cu^{2+} is loaded onto the surface of MXene nanosheets via electrostatic adsorption to prepare an MXene@Cu nanocomposite. The synergy of MXene nanosheets and Cu nanoparticles could lead to the formation of a stable protective film on the surface of the friction pair and thus provide excellent tribological performance [84]. Compared with MoS_2, tungsten-doped amorphous carbon (a-C:H:W) and hydrogen-free, more graphitelike amorphous carbon (a-C), MXene can significantly reduce the friction coefficient and wear rate of composites during the dry friction process [85]. However, due to the presence of the -OH, -O and -F functional groups on the surface, MXene has high surface energy, as well as poor dispersion and stability, in polar polymers or weakly polar polymers [86]. MXene was modified with tetradecylphosphonic acid and Poly[2(Perfluorooctyl)ethyl methacrylate] to improve its dispersibility in the lubrication oil, enhance its adsorption capacity on the substrate surface, and reduce the shear effect in the contact zone [5,87].

MXene has metal conductivity and colloidal processing properties, which can be used to enhance the friction and conductivity of hydrogels and enable broad application prospects in the field of temperature sensors and light-responsive soft robots [88,89]. Hydrogels can be used as drug carriers, coating drug molecules, reducing immune response and extending drug stability and storage life [90]. In order to realize the intelligent response of drug release, Yan et al. prepared a responsive nanofiber using MXene and hydrogel, which enhanced the dispersion of the hydrogel in a fiber membrane, and they controlled the drug release ability of the fiber membrane through light intensity [91]. MXene also has more active groups on its surface, meaning it can be used as a hydrogel crosslinking agent to optimize the structure, mechanical strength and tribolgical behavior of hydrogels. The tensile strength, toughness and elongation at break of the synthesized hydrogel with the addition of MXene are 0.251 MPa, 0.895 MJ m^{-3}, and 560.82%, respectively [92]. The formation of hydrogen bonds between MXene and the PVA molecular chains substantially fortifies the structure and hydration capacity of a hydrogel network, as depicted in Figure 7 [93]. The presence of reactive functional groups on the surface of MXene nanosheets, which share a graphene-like structure, allows for effective interaction with the hydrogel's molecular chains. This interaction not only reinforces the mechanical attributes of the hydrogels, but also enhances their lubricating properties, thereby contributing to a more robust and versatile material. Ye et al. added MXene and dopamine to a poly PEGDA–methylacrylic anhydride–gelatin hydrogel to synthesize a bionic heart patch with high electrical conductivity and excellent biocompatibility. The mechanical properties of the composite hydrogel containing MXene were enhanced by 60% [94]. However, using MXene as a single additive can only improve the mechanical properties of hydrogels in a limited way. MXene and nanocellulose were used to synthesize composite nanoadditives; here, nanocellulose could improve the dispersibility of MXene in hydrogels, and its synergy with MXene could promote the cross-linking of hydrogel networks [95].

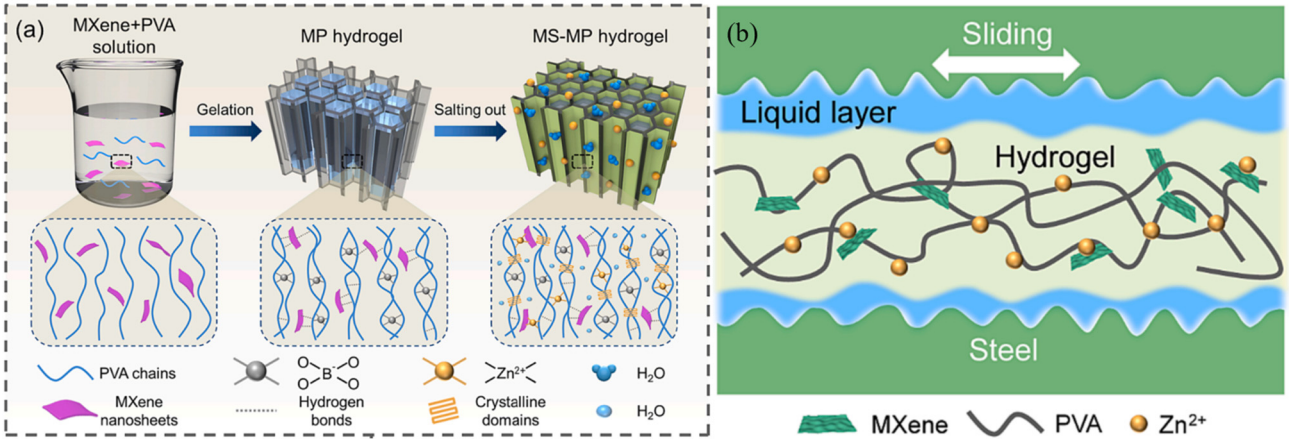

Figure 7. Schematic diagram of MXene-based hydrogels. (**a**) Multi-crosslinked and solid–liquid composite lubricating hydrogel; (**b**) the lubrication mechanism of hydrogels with MXene [93], copyright (2023), with permission from Elsevier.

A variety of synthesis methods have been proposed to improve the surface chemical properties of MXene, such as reactions between metals and metal halides, or selective etching in a mixture. Although it is theoretically possible to synthesize new MXene materials by changing M, X, n and Tx inserts, more oxidative impurities will be generated through etching, which will affect the microstructural and macroscopic properties of MXene, and lead to the production of toxic substances during synthesis processes, thus causing pollution to the human body and the environment [96,97]. The available uniform surface terminations of MXenes, including oxygen, imido group, sulfur, chlorine, selenium, bromine and tellurium, were also controlled using computational studies or various synthetic methods [98]. In addition, a universal 4D printing technology was used to prepare MXene-family hydrogels, such as Nb_2CT_x, $Ti_3C_2T_x$, and $Mo_2Ti_2C_3T_x$. The 4D-printed MXene hydrogel that was obtained could be used to create 3D porous architectures, with large specific surface areas, high electrical conductivities, and excellent mechanical properties [99].

Numerous studies have elucidated the considerable potential of MXene materials to enhance mechanical and tribological properties when employed as nanofillers in conjunction with other two-dimensional materials or nanoparticles. The unique elemental composition, surface terminations, and structural attributes of MXenes are the factors determining their mechanical characteristics [100]. The weak secondary interlayer bonding between adjacent layers of various combinations and forms of MXenes will result in a low shear resistance, which makes them promising for use in tribological applications [100]. Moreover, applying MXenes on different surfaces could decrease the interfacial adhesion, and their chemical reactivity at high pressures and temperatures might lead to the formation of a tribolayer in tribological contacts. The formed tribofilm tends to provide good substrate adhesion, as well as long-term low-friction and low-wear performance [101]. In addition, a variety of surface terminations on the outer surfaces of MXenes can be functionalized to improve their dispersion stability, oxidation resistance and compatibility with other matrix materials in composites, thus leading to an enhanced tribological performance [102].

2.5. Other 2D Materials

Recently, some other 2D nanoparticles with various functions have been under development [103]. Cadmium sulfide (CdS) photocatalytic nanoparticles were incorporated as a reinforced material into a P(AA-AM) composite hydrogel [104]. Increasing amounts of CdS could significantly enhance the mechanical strength of the hydrogel from 0.445 MPa to 1.014 MPa. The P(AA-AM)@CdS nanocomposite hydrogel also exhibited strong synergistic adsorption and photocatalytic degradation clearance effects with methylene blue. Thus, the introduction of CdS photocatalytic nanoparticles may enable the efficient enhancement of the mechanical properties of bifunctional hydrogel materials. Bioactive glass nanoparticles

(BG) with particle sizes of 12 and 25 nm were incorporated into Alginate–gelatin (Alg-Gel) hydrogel [105]. The nanocomposite hydrogel exhibited significantly enhanced stiffness and printability with increasing BG concentrations, as well as cellular proliferation and adhesion in the bioprinted constructs. The introduction of BG also did not significantly contribute to the highly porous structure and biodegradation of Alg-Gel hydrogel, which might ground its potential application in extrusion-based bioprinting. Dai et al. [106] used gold nanorods (AuNRs) to prepare a tough nanocomposite hydrogel with a designable gradient network structure via a facile post-photo regulation strategy. The photothermal effects of AuNRs could locally improve the typical yielding and forced elastic deformation of hydrogels with a kirigami structure by near-infrared light irradiation at room temperature, because the treated regions show better resistance to crack advancement. These tough hydrogels with programmable gradient structures and mechanics have many potential applications, such as in structural elements and biological devices. Wang et al. [107] prepared a novel hybrid hydrogel based on PVA, borax and poly-dopamine particles (PDAPs). With the increasing content of PDAPs, the hybrid hydrogels exhibited a higher tensile strength from 5.86 MPa to 16.71 MPa, and a better self-healing efficiency of 114%, after contact at room temperature for 10 min. This nanoparticle-induced strengthening might expand its potential applications, such as into electrical skin, tissue engineering, drug delivery, 3D printing and soft robots areas. Cellulose nanowafers (CNWs) were added by Du et al. [108] to the PAAM/Xanthan gum-Al^{3+} DN hydrogel. The prepared hydrogel showed a maximum stress of 0.14 MPa when the elongation at break was 707.1%. The improved mechanical properties and self-recovery were attributed to the combination between the PAAM and the CNWs. The developed hydrogel with high tensile strength showed great potential for use in various applications, such as in wearable sensors for the detection of human movement. Functionalized silicon nanoparticles (SiNPs) were used by Yang et al. [109] as the cross-linker to synthesize a novel organic–inorganic hybrid bilayer PNIPAm@PAAm hydrogel. The introduction of the doped SiNPs could considerably improve the rigidity of a PAAm-type hydrogel network, leading to excellent tensile and compressive strength (Figure 8). The low cost and excellent biocompatibility of the SiNPs could expand their potential use in future applications in smart hydrogel materials. Li et al. [110] used carboxyl-modified Fe_3O_4 nanoparticles as a photothermal agent to synthesize a carboxymethyl chitosans–Fe_3O_4–acrylamide (CMCS-Fe_3O_4-AM) hydrogel with good drug loading and antibacterial properties. The introduction of carboxyl-modified Fe_3O_4 could significantly change the structural density, mechanical strength, and photothermal properties of the nano-composite hydrogel. This research might provide a novel design for new hydrogels with good mechanical properties, controllable crosslink density and photothermal properties. Lu et al. [111] used TEMPO-oxidized cellulose nanofibers (TOCNs) as a filler to develop a novel TOCN/PAAM nanocomposite hydrogel. TOCNs with high strength and ultra-high aspect ratio could improve the energy dissipation capability (9.68 MJ m^{-3} at 60% strain), viscoelasticity (51.1 kPa) and self-recovery rate (about 93.2% after 30 min recovery) of polyacrylamide (PAAM) hydrogel. This nanocomposite hydrogel with good shape memory properties and excellent mechanical strength provides promising prospects for use in intelligent biomaterials used in soft actuators, biomedicine and sensory applications. Biocompatible micro/nanoparticles containing various ratios of Ca^{2+} and Mg^{2+} with sizes ranging from 1 to 8 μm were mixed with gellan gum (GG) solution to form a self-hardening multifunctional hydrogel [112]. The Ca^{2+}/Mg^{2+} particles could be efficiently bound to GG polymer chains for the enhancement of the macro-Young's modulus of the hydrogel from 2 kPa up to 100 kPa. This hydrogel with hydro-magnesite particles also exhibited a higher cell viability and greater hydroxyapatite production. This research opens new avenues for developing injectable reconstruction materials for use in biomedical applications related to bone regeneration.

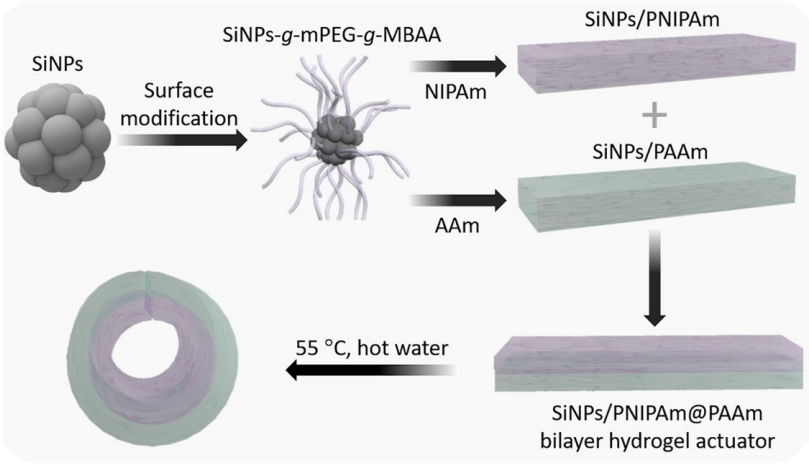

Figure 8. Synthetic procedure and structural illustration of the SiNPs/PNIPAm@PAAm bilayer hydrogel [109], copyright (2021), with permission from Elsevier.

It is here shown that 2D nanomaterials can interact with hydrogel polymer chains to synthesize nanocomposite hydrogels with excellent mechanical properties. Table 2 shows the mechanical and tribological properties of hydrogels reinforced with various 2D nanomaterials. Different types and mass fractions of these 2D nanomaterials affect the macroscopic properties of synthetic nanocomposite hydrogels. Zhang found that the mechanical properties of nanocomposite hydrogels began to decline when the mass fraction of GO was greater than 5.0 wt. %, mainly due to the polymerization inside the hydrogel, caused by an excessive amount of GO [42].

Table 2. Mechanical properties of hydrogels reinforced by 2D nanomaterials with optimal content.

2D Nanomaterials	Hydrogel	Maximum Mechanical Strength	Friction Coefficient	Concentration/Weight Percent
GO	PSBMA [23]	Compressive strength: 0.08 MPa~0.36 MPa Tensile strength: 50.7 kPa~151.9 kPa	0.006~0.03	0.005~0.025 wt. %
	PVA-PNIPA [39]	Compressive strength: 1.5 MPa~4.1 MPa		10~25 mg
	CS [43]	Tensile strength: 4.37 MPa~20.96 MPa Young's modulus: 0.122 to 0.364 MPa		0.1~0.5 wt. %
	PAAm [49]	Tensile strength: 10 MPa~50 MPa	0.05~0.12	0.2~2 wt. %
	PVA-PEG-HA [50]	Compressive strength: 1.95 MPa~4.79 MPa		1.5 wt. %
	PVA-PAA-PDA [51]	Compressive modulus: 1.12 MPa~2.53 MPa Young's modulus: 0.051 GPa~0.058 GPa	0.05~0.12	0.1~1 wt. %
	PVA [54]	Compressive strength: 0.29 MPa~0.42 MPa Tensile strength: 0.19 MPa~0.27 MPa	0.05~0.20	0~0.09 wt. %
h-BN	PAA [56]	Stiffness: 17.9 MPa, toughness: 10.5 MJ m^{-3}		0.1~1.0 mg mL^{-1}
	PU [58]	Young's modulus: 1632 kPa~2776 kPa		0.03~0.18 wt.%
	PAAm [59]	Compressive strength: ~8 MPa		0.1~2.5 mg mL^{-1}
	Clay- PNIPAM [60]	Compressive strength: 30 kPa~200 kPa Tensile strength: 17 kPa~40 kPa		0.04~0.32 wt. %
BP	PEA-GelMA [73]	Compressive strength: ~0.15 MPa Compressive moduli: 0.3 MPa~0.9 MPa		40 wt. %
	NS-CS coating [74]	Compressive moduli: 247.9 MPa~745.4 MPa Tensile moduli: 235 MPa~644 MPa		50 mg
MXene	oligo[poly(ethylene glycol) fumarate](OPF) [113]	Compression modulus: 497 kPa~734.5 kPa		0.1~1 mg mL^{-1}
	PAM [90]	Compressive strength: 400.6 kPa~819.4 kPa		0.0145~0.0436 wt. %
	PAA-PAM-TA [92]	Tensile strength: 0.251 ± 0.05 MPa		0.075 g
	PVA [93]		0.14~0.18	1~10 mg mL^{-1}
	Cryogel [94]	Compression modulus: 2.24 kPa~9.65 kPa		0.4~1.6 mg

3. Challenges and Perspectives

Hydrogels infused with 2D materials as nanofillers show immense potential utility in bioapplications, thanks to their improved mechanical and tribological characteristics. While significant advancements have been made in this field over the years, there remain a number of challenges that must be addressed to enable further progress in both scientific research and engineering applications:

- The dispersion stability of 2D materials in water-based solutions is governed by the surface energy, which significantly affects their internal interaction with polymer molecular chains of hydrogels [113]. Hence, the challenge lies in optimizing hydrogel systems to achieve a high load-bearing capacity and reduced friction at the lowest possible particle concentration. This aspect requires additional research if we are to realize the practical applications of these systems;
- The synthesis of 2D nanomaterials still involves some limitations. For example, the large-scale synthesis of 2D materials with precisely controlled nanostructures is difficult to realize. Advanced techniques and equipment for the preparation of 2D materials should be further developed.
- There is still a lack of extensive research on the optimization of basic parameters of 2D nanomaterials to be used as promising fillers for the feasible functional design of hydrogels. For example, the influence of some features of 2D materials, including the layer number, lateral size [114], types, and the concentration of functional groups, on the mechanical and tribological behaviors of hydrogels for specified bioapplications remains unclear. An in-depth investigation of the fundamental mechanisms and advanced techniques guiding the design and application of 2D materials as nanofillers in hydrogels is required in the future;
- The strengthening and lubrication mechanisms of 2D materials used as nanofillers of hydrogels still need to be further elucidated, and this should be based on a full understanding of the fundamental properties of both the 2D materials and the polymeric hydrogel matrix;
- The biocompatibility of hydrogels incorporating 2D materials as nanofillers necessitates a more rigorous and systematic investigation. This should encompass an extensive evaluation of multiple factors, including cytotoxicity, neurotoxicity, genotoxicity, and others, to ensure safety and efficacy over an extended period of service;
- Furthermore, the ongoing development of 2D nanomaterials opens up new avenues for enhancing the mechanical and tribological properties of nanocomposite hydrogels. For instance, the tribological attributes of nitride-MXenes have not been thoroughly investigated, despite their known superior mechanical properties [115–117]. Additionally, the potential synergistic effects of integrating diverse 2D nanomaterials into hydrogels are an area that is ripe for exploration, as there is insufficient research on this combined approach to offer comprehensive data and permit systematic studies. Moreover, incorporating novel "non-layered" 2D materials [118–121] as nanofillers could introduce distinctive characteristics to nanocomposite hydrogels, offering a new dimension of performance and functionality.

4. Conclusions

This review has underscored the significance of incorporating typical 2D nanomaterials in order to enhance the mechanical and tribological attributes of polymer hydrogels. It also highlights key challenges that must be addressed in future research. The objective is to offer a valuable resource for the design and advancement of hydrogels fortified with various functional 2D materials. We anticipate that these 2D nanomaterials will be pivotal in engineering composite hydrogels, and trust that the insights presented here will serve as a foundation for developing multifunctional hydrogels across a wide range of applications.

Author Contributions: Writing—original draft preparation, H.G. and Z.W.; funding acquisition, Y.L.; writing—review and editing, Y.L., J.Z. and Y.Q. All authors have read and agreed to the published version of the manuscript.

Funding: This work was financially supported by the National Natural Science Foundation of China (grant number 52005287), Beijing Institute of Technology Research Fund Program for Young Scholars, Tribology Science Fund of State Key Laboratory of Tribology in Advanced Equipment (SKLT) (No. SKLTKF21B14), and Young Elite Scientists Sponsorship Program by BAST (grant number BYESS2023288).

Data Availability Statement: The data presented in this study are available on request from the corresponding author.

Conflicts of Interest: Yi Qian was employed by Beijing Montagne Medical Device Co., Ltd. The remaining authors declare that the research was conducted in the absence of any commercial or financial relationships that could be construed as a potential conflict of interest.

References

1. Bonyadi, S.Z.; Demott, C.J.; Grunlan, M.A.; Dunn, A.C. Cartilage-like Tribological Performance of Charged Double Net-work Hydrogels. *J. Mech. Behav. Biomed. Mater.* **2021**, *114*, 104202. [CrossRef] [PubMed]
2. Feng, S.; Li, J.; Li, X.; Wen, S.; Liu, Y. Synergy of Phospholipid and Hyaluronan Based Super-Lubricated Hydrogels. *Appl. Mater. Today* **2022**, *27*, 101499. [CrossRef]
3. Zhao, X.; Xiong, D.; Liu, Y. Improving Surface Wettability and Lubrication of Polyetheretherketone (PEEK) by Combining with Polyvinyl Alcohol (PVA) Hydrogel. *J. Mech. Behav. Biomed. Mater.* **2018**, *82*, 27–34. [CrossRef] [PubMed]
4. Song, H.S.; Kwon, O.S.; Kim, J.H.; Conde, J.; Artzi, N. 3D hydrogel scaffold doped with 2D graphene materials for biosensors and bioelectronics. *Biosens. Bioelectron.* **2017**, *89*, 187–200. [CrossRef] [PubMed]
5. Chen, Y.; Song, J.; Wang, S.; Liu, W. Cationic Modified PVA Hydrogels Provide Low Friction and Excellent Mechanical Properties for Potential Cartilage and Orthopedic Applications. *Macromol. Biosci.* **2023**, *23*, 2200275. [CrossRef]
6. Lust, S.T.; Hoogland, D.; Norman, M.D.A.; Kerins, C.; Omar, J.; Jowett, G.M.; Yu, T.T.L.; Yan, Z.; Xu, J.Z.; Marciano, D.; et al. Selectively Cross-Linked Tetra-PEG Hydrogels Provide Control over Mechanical Strength with Minimal Impact on Diffusivity. *ACS Biomater. Sci. Eng.* **2021**, *7*, 4293–4304. [CrossRef] [PubMed]
7. Chen, S.; Huang, J.; Zhou, Z.; Chen, Q.; Hong, M.; Yang, S.; Fu, H. Highly Elastic Anti-Fatigue and Anti-Freezing Conductive Double Network Hydrogel for Human Body Sensors. *Ind. Eng. Chem. Res.* **2021**, *60*, 6162–6172. [CrossRef]
8. Wang, Z.; Meng, F.; Zhang, Y.; Guo, H. Low-Friction Hybrid Hydrogel with Excellent Mechanical Properties for Simulating Articular Cartilage Movement. *Langmuir* **2023**, *39*, 2368–2379. [CrossRef]
9. Li, Z.; Zhang, X.; Cheng, H.; Liu, J.; Shao, M.; Wei, M.; Evans, D.; Zhang, H.; Duan, X. Confined Synthesis of 2D Nanostructured Materials toward Electrocatalysis. *Adv. Energy Mater.* **2020**, *10*, 1900486. [CrossRef]
10. Kim, H.G.; Lee, H. Atomic Layer Deposition on 2D Materials. *Chem. Mater.* **2017**, *29*, 3809–3826. [CrossRef]
11. Chen, P.; Wu, Z.; Huang, Q.; Ji, S.; Weng, Y.; Wu, Z.; Ma, Z.; Chen, X.; Weng, M.; Fu, R.; et al. A quasi-2D material CePO4 and the self-lubrication in micro-arc oxidized coatings on Al alloy. *Tribol. Int.* **2019**, *138*, 157–165. [CrossRef]
12. Uzoma, P.C.; Hu, H.; Khadem, M.; Penkov, O.V. Tribology of 2D nanomaterials: A review. *Coatings* **2020**, *10*, 897. [CrossRef]
13. Rong, C.; Su, T.; Li, Z.; Chu, T.; Zhu, M.; Yan, Y.; Zhang, B.; Xuan, F. Elastic properties and tensile strength of 2D $Ti_3C_2T_x$ MXene monolayers. *Nat. Commun.* **2024**, *15*, 1566. [CrossRef] [PubMed]
14. Novoselov, K.S.; Fal'ko, V.I.; Colombo, L.; Gellert, P.R.; Schwab, M.G.; Kim, K. A roadmap for graphene. *Nature* **2012**, *490*, 192–200. [CrossRef] [PubMed]
15. Huang, S.; Mutyala, K.C.; Sumant, A.V.; Mochalin, V.N. Achieving superlubricity with 2D transition metal carbides (MXenes) and MXene/graphene coatings. *Mater. Today Adv.* **2021**, *9*, 100133. [CrossRef]
16. Rasul, M.G.; Kiziltas, A.; Arfaei, B.; Shahbazian-Yassar, R. 2D boron nitride nanosheets for polymer composite materials. *Npj 2D Mater. Appl.* **2021**, *5*, 56. [CrossRef]
17. Wu, H.; Yin, S.; Du, Y.; Wang, L.; Wang, H. An investigation on the lubrication effectiveness of MoS_2 and BN layered materials as oil additives using block-on-ring tests. *Tribol. Int.* **2020**, *151*, 106516. [CrossRef]
18. Tanjil, M.R.E.; Jeong, Y.; Yin, Z.; Panaccione, W.; Wang, C.M. Angstrom-Scale, Atomically Thin 2D Materials for Corrosion Mitigation and Passivation. *Coatings* **2019**, *9*, 133. [CrossRef]
19. Xia, M. 2D Materials-Coated Plasmonic Structures for SERS Applications. *Coatings* **2018**, *8*, 137. [CrossRef]
20. Liu, Y.; Li, J.; Li, J.; Yi, S.; Ge, X.; Zhang, X.; Luo, J. Shear-Induced Interfacial Structural Conversion Triggers Macroscale Superlubricity: From Black Phosphorus Nanoflakes to Phosphorus Oxide. *ACS Appl. Mater. Interfaces* **2021**, *13*, 31947–31956. [CrossRef]
21. Zheng, Y.; Hong, X.; Wang, J.; Feng, L.; Fan, T.; Guo, R.; Zhang, H. 2D Nanomaterials for Tissue Engineering and Regenerative Nanomedicines: Recent Advances and Future Challenges. *Adv. Healthc. Mater.* **2021**, *10*, 2001743. [CrossRef] [PubMed]

22. Marian, M.; Berman, D.; Nečas, D.; Emami, N.; Ruggiero, A.; Rosenkranz, A. Roadmap for 2D materials in biotribological/biomedical applications—A review. *Adv. Colloid Interface Sci.* **2022**, *307*, 102747. [CrossRef]
23. Wang, Z.; Li, J.; Jiang, L.; Xiao, S.; Liu, Y.; Luo, J. Zwitterionic Hydrogel Incorporated Graphene Oxide Nanosheets with Improved Strength and Lubricity. *Langmuir* **2019**, *35*, 11452–11462. [CrossRef] [PubMed]
24. Urade, A.R.; Lahiri, I.; Suresh, K.S. Graphene Properties, Synthesis and Applications: A Review. *J. Miner. Met. Mater. Soc. (TMS)* **2023**, *75*, 614–630. [CrossRef] [PubMed]
25. Jiang, H.; Zheng, L.; Liu, Z.; Wang, X. Two-dimensional materials: From mechanical properties to flexible mechanical sensors. *InfoMat* **2020**, *2*, 1077–1094. [CrossRef]
26. Suk, J.; Piner, R.; An, J.; Ruoff, R. Mechanical Properties of Monolayer Graphene Oxide. *ACS Nano* **2010**, *4*, 6557–6564. [CrossRef] [PubMed]
27. Falin, A.; Cai1, Q.; Santos, E.; Scullion, D.; Qian, D.; Zhang, R.; Yang, Z.; Huang, S.; Watanabe, K.; Taniguchi, T.; et al. Mechanical properties of atomically thin boron nitride and the role of interlayer interactions. *Nat. Commun.* **2017**, *8*, 15815. [CrossRef]
28. Jiang, J.; Park, H. Mechanical properties of single-layer black phosphorus. *J. Phys. D Appl. Phys.* **2014**, *47*, 385304. [CrossRef]
29. Li, L.; Yang, J. On mechanical behaviors of fewlayer black phosphoru. *Sci. Rep.* **2018**, *8*, 3227. [CrossRef]
30. Liu, Y.; Ge, X.; Li, J. Graphene lubrication. *Appl. Mater. Today* **2020**, *20*, 100662. [CrossRef]
31. Ge, X.; Chai, Z.; Shi, Q.; Liu, Y.; Wang, W. Graphene superlubricity: A review. *Friction* **2023**, *11*, 1953–1973. [CrossRef]
32. Mao, J.; Zhao, J.; Wang, W.; He, Y.; Luo, J. Influence of the micromorphology of reduced graphene oxide sheets on lubrication properties as a lubrication additive. *Tribol. Int.* **2018**, *119*, 614–621. [CrossRef]
33. Liang, H.; Xu, M.; Bu, Y.; Chen, B.; Zhang, Y.; Fu, Y.; Xu, X.; Zhang, J. Confined interlayer water enhances solid lubrication per-formances of graphene oxide films with optimized oxygen functional groups. *Appl. Surf. Sci.* **2019**, *485*, 64–69. [CrossRef]
34. Gupta, B.; Kumar, N.; Panda, K.; Dash, S.; Tyagi, A.K. Energy efficient reduced graphene oxide additives: Mechanism of effective lubrication and antiwear properties. *Sci. Rep.* **2016**, *6*, 18372. [CrossRef]
35. Chen, L.; Tu, N.; Wei, Q.; Liu, T.; Li, C.; Wang, W.; Li, J.; Lu, H. Inhibition of cold-welding and adhesive wear occurring on sur-face of the 6061 aluminum alloy by graphene oxide/polyethylene glycol composite water-based lubricant. *Surf. Inter-Face Anal.* **2021**, *54*, 218–230. [CrossRef]
36. Cheng, Y.H.; Cheng, S.J.; Chen, H.H.; Hsu, W.C. Development of injectable graphene oxide/laponite/gelatin hydrogel con-taining Wharton's jelly mesenchymal stem cells for treatment of oxidative stress-damaged cardiomyocytes. *Colloids Surf. B Biointerfaces* **2022**, *209*, 112150. [CrossRef]
37. Qiao, K.; Guo, S.; Zheng, Y.; Xu, X.; Meng, H.; Peng, J.; Fang, Z.; Xie, Y. Effects of graphene on the structure, properties, electro-response behaviors of GO/PAA composite hydrogels and influence of electro-mechanical coupling on BMSC differentiation. *Mater. Sci. Eng. C Mater. Biol. Appl.* **2018**, *93*, 853–863. [CrossRef]
38. Hou, Y.; Jin, M.; Liu, Y.; Jiang, N.; Zhang, L.; Zhu, S. Biomimetic construction of a lubricious hydrogel with robust mechanics via polymer chains interpenetration and entanglement for TMJ disc replacement. *Chem. Eng. J.* **2023**, *460*, 141731. [CrossRef]
39. Lei, Y.; Zhang, G.; Li, H. Thermal-responsive nanocomposite hydrogel based on graphene oxide-polyvinyl alcohol/poly (N-isopropylacrylamide). *IOP Conf. Ser. Mater. Sci. Eng.* **2017**, *274*, 012115. [CrossRef]
40. Li, G.; Zhao, Y.; Zhang, L.; Gao, M.; Kong, Y.; Yang, Y. Preparation of graphene oxide/polyacrylamide composite hydrogel and its effect on Schwann cells attachment and proliferation. *Colloids Surf. B Biointerfaces* **2016**, *143*, 547–556. [CrossRef] [PubMed]
41. Zhu, P.; Hu, M.; Deng, Y.; Wang, C. One-Pot Fabrication of a Novel Agar-Polyacrylamide/Graphene Oxide Nanocomposite Double Network Hydrogel with High Mechanical Properties. *Adv. Eng. Mater.* **2016**, *18*, 1799–1807. [CrossRef]
42. Zhang, Y.; Zhang, M.; Jiang, H.; Shi, J.; Li, F.; Xia, Y.; Zhang, G.; Li, H. Bio-inspired layered chitosan/graphene oxide nanocomposite hydrogels with high strength and pH-driven shape memory effect. *Carbohydr. Polym.* **2017**, *177*, 116–125. [CrossRef]
43. Nath, J.; Chowdhury, A.; Dolui, S.K. Chitosan/graphene oxide-based multifunctional pH-responsive hydrogel with significant mechanical strength, self-healing property, and shape memory effect. *Adv. Polym. Technol.* **2018**, *37*, 3665–3679. [CrossRef]
44. Zhang, S.; Gong, X.; Yu, R.; Xing, Q.; Xu, L.; Wang, Z. Self-lubrication and wear-resistance mechanism of graphene-modified coatings. *Ceram. Int.* **2020**, *46*, 15915–15924.
45. Wang, Z.; Hao, Z.; Yang, C.; Wang, H.; Huang, C.; Zhao, X.; Pan, Y. Ultra-sensitive and rapid screening of acute myocardial in-farction using 3D-affinity graphene biosensor. *Cell Rep. Phys. Sci.* **2022**, *3*, 100855. [CrossRef]
46. Yang, J.; Hu, D.; Li, W.; Jia, Y.; Li, P. Formation mechanism of zigzag patterned P(NIPAM-co-AA)/CuS composite microspheres by in situ biomimetic mineralization for morphology modulation. *RSC Adv.* **2021**, *11*, 37904. [CrossRef]
47. Wang, B.; Yuan, S.; Xin, W.; Chen, Y.; Fu, Q.; Li, L.; Jiao, Y. Synergic adhesive chemistry-based fabrication of BMP-2 immobilized silk fibroin hydrogel functionalized with hybrid nanomaterial to augment osteogenic differentiation of rBMSCs for bone defect repair. *Int. J. Biol. Macromol.* **2021**, *192*, 407–416. [CrossRef]
48. Meng, Y.; Ye, L.; Coates, P.; Twigg, P. In Situ Cross-Linking of Poly(vinyl alcohol)/Graphene Oxide–Polyethylene Glycol Nanocomposite Hydrogels as Artificial Cartilage Replacement: Intercalation Structure, Unconfined Compressive Behavior, and Biotribological Behaviors. *J. Phys. Chem. C* **2018**, *122*, 3157–3167. [CrossRef]
49. Wang, C.; Bai, X.; Guo, Z.; Dong, C.; Yuan, C. A strategy that combines a hydrogel and graphene oxide to improve the water-lubricated performance of ultrahigh molecular weight polyethylene. *Compos. Part A Appl. Sci. Manuf.* **2021**, *141*, 106207. [CrossRef]

50. Cao, J.; Meng, Y.; Zhao, X.; Ye, L. Dual-Anchoring Intercalation Structure and Enhanced Bioactivity of Poly(vinyl alcohol)/Graphene Oxide–Hydroxyapatite Nanocomposite Hydrogels as Artificial Cartilage Replacement. *Ind. Eng. Chem. Res.* **2020**, *59*, 20359–20370. [CrossRef]
51. Wang, C.; Zhu, K.; Gao, Y.; Han, S.; Ju, J.; Ren, T.; Zhao, X. Multifunctional GO-based hydrogel coating on Ti-6Al-4 V Alloy with enhanced bioactivity, anticorrosion and tribological properties against cortical bone. *Tribol. Int.* **2023**, *184*, 108423. [CrossRef]
52. Liu, L.; Xiao, L.; Li, M.; Zhang, X.; Chang, Y.; Shang, L.; Ao, Y. Effect of hexagonal boron nitride on high-performance polyether ether ketone composites. *Colloid Polym. Sci.* **2016**, *294*, 127–133. [CrossRef]
53. Belyaeva, L.; Ludwig, C.; Lai, Y.; Chou, C.; Shih, C. Uniform, Strain-Free, Large-Scale Graphene and h-BN Monolayers Enabled by Hydrogel Substrates. *Small* **2023**, *20*, 2307054. [CrossRef]
54. Jing, L.; Li, H.; Tay, Y.; Sun, B.; Tsang, S.H.; Cometto, O.; Lin, J.; Teo, E.; Tok, A. Biocompatible Hydroxylated Boron Nitride Nanosheets/Polyvinyl Alcohol Interpenetrating Hydrogels with Enhanced Mechanical and Thermal Responses. *ACS Nano* **2017**, *11*, 3742–3751. [CrossRef]
55. Yang, N.; Ji, H.; Jiang, X.; Qu, X.; Zhang, X.; Zhang, Y.; Liu, B. Preparation of Boron Nitride Nanoplatelets via Amino Acid Assisted Ball Milling: Towards Thermal Conductivity Application. *Nanomaterials* **2020**, *10*, 1652. [CrossRef]
56. Xue, S.; Wu, Y.; Guo, M.; Liu, D.; Zhang, T.; Lei, W. Fabrication of Poly(acrylic acid)/Boron Nitride Composite Hydrogels with Excellent Mechanical Properties and Rapid Self-Healing Through Hierarchically Physical Interactions. *Nanoscale Res. Lett.* **2018**, *13*, 393. [CrossRef]
57. Jiang, H.; Wang, Z.; Geng, H.; Song, X.; Zeng, H.; Zhi, C. Highly Flexible and Self-Healable Thermal Interface Material Based on Boron Nitride Nanosheets and a Dual Cross-linked Hydrogel. *ACS Appl. Mater. Interfaces* **2017**, *9*, 10078–10084. [CrossRef]
58. Liu, F.; Han, R.; Naficy, S.; Casillas, G.; Sun, X.; Huang, Z. Few-Layered Boron Nitride Nanosheets for Strengthening Polyurethane Hydrogels. *ACS Appl. Nano Mater.* **2021**, *4*, 7988–7994. [CrossRef]
59. Hu, X.; Liu, J.; He, Q.; Meng, Y.; Cao, L.; Sun, Y.; Chen, J.; Lu, F. Aqueous compatible boron nitride nanosheets for high-performance hydrogels. *Nanoscale* **2016**, *8*, 4260–4266. [CrossRef]
60. Tong, X.; Du, L.; Xu, Q. Tough, Adhesive and Self-Healing Conductive 3D Network Hydrogel of Physically Linked Functionalized-Boron Nitride/Clay/Poly(N-isopropylacrylamide). *J. Mater. Chem. A* **2018**, *6*, 3091–3099. [CrossRef]
61. Goncu, Y.; Ay, N. Boron Nitride's Morphological Role in the Design of Injectable Hyaluronic Acid Based Hybrid Artificial Synovial Fluid. *ACS Biomater. Sci. Eng.* **2023**, *9*, 6345–6356. [CrossRef] [PubMed]
62. Fan, L.; Zhang, X.; Liu, X.; Sun, B.; Li, L.; Zhao, Y. Responsive Hydrogel Microcarrier-Integrated Microneedles for Versatile and Controllable Drug Delivery. *Adv. Healthc. Mater.* **2021**, *10*, 2002249. [CrossRef]
63. Yang, G.; Wan, X.; Gu, Z.; Zeng, X.; Tang, J. Near infrared photothermal-responsive poly(vinyl alcohol)/black phosphorus com-posite hydrogels with excellent on-demand drug release capacity. *J. Mater. Chem. B* **2018**, *6*, 1622–1632. [CrossRef]
64. Lv, Y.; Wang, W.; Xie, G.; Luo, J. Self-Lubricating PTFE-Based Composites with Black Phosphorus Nanosheets. *Tribol. Lett.* **2018**, *66*, 61. [CrossRef]
65. Sun, X.; Yu, C.; Zhang, L.; Cao, J.; Kaleli, E.H.; Xie, G. Tribological and Antibacterial Properties of Polyetheretherketone Composites with Black Phosphorus Nanosheets. *Polymers* **2022**, *14*, 1242. [CrossRef]
66. Wu, S.; He, F.; Xie, G.; Bian, Z.; Ren, Y.; Liu, X.; Yang, H.; Guo, D.; Zhang, L.; Wen, S.; et al. Super-Slippery Degraded Black Phosphorus/Silicon Dioxide Interface. *ACS Appl. Mater. Interfaces* **2020**, *12*, 7717–7726. [CrossRef]
67. Luo, Z.; Yu, J.; Xu, Y.; Xi, H.; Cheng, G.; Yao, L.; Song, R.; Dearn, K.D. Surface characterization of steel/steel contact lubricated by PAO6 with novel black phosphorus nanocomposites. *Friction* **2020**, *9*, 723–733. [CrossRef]
68. Tang, G.; Su, F.; Xu, X.; Chu, P.K. 2D black phosphorus dotted with silver nanoparticles: An excellent lubricant additive for tribological applications. *Chem. Eng. J.* **2020**, *392*, 123631. [CrossRef]
69. Wang, W.; Gong, P.; Hou, T.; Wang, Q.; Gao, Y.; Wang, K. Tribological performances of BP/TiO_2 nanocomposites as water-based lubrication additives for titanium alloy plate cold rolling. *Wear* **2022**, *204278*, 494–495. [CrossRef]
70. Xu, Y.; Yu, J.; Dong, Y.; You, T.; Hu, X. Boundary Lubricating Properties of Black Phosphorus Nanosheets in Polyalphaolefin Oil. *J. Tribol.* **2019**, *141*, 072101. [CrossRef]
71. Wang, Q.; Hou, T.; Wang, W.; Zhang, G.; Gao, Y.; Wang, K. Tribological behavior of black phosphorus nanosheets as water-based lubrication additives. *Friction* **2021**, *10*, 374–387. [CrossRef]
72. Liu, W.; Zhu, Y.; Tao, Z.; Chen, Y.; Zhang, L.; Dong, A. Black Phosphorus-Based Conductive Hydrogels Assisted by Electrical Stimulus for Skin Tissue Engineering. *Adv. Healthc. Mater.* **2023**, *12*, 2301817. [CrossRef]
73. Du, C.; Huang, W. Progress and prospects of nanocomposite hydrogels in bone tissue engineering. *Nanocomposites* **2022**, *8*, 102–124. [CrossRef]
74. He, M.; Zhu, C.; Sun, D.; Liu, Z.; Du, M.; Huang, Y.; Huang, L.; Wang, J.; Liu, L.; Li, Y.; et al. Layer-by-layer assembled black phosphorus/chitosan composite coating for multi-functional PEEK bone scaffold. *Compos. Part B Eng.* **2022**, *246*, 110266. [CrossRef]
75. Malaki, M.; Varma, R.S. Mechanotribological Aspects of MXene-Reinforced Nanocomposites. *Adv. Mater.* **2020**, *32*, 2003154. [CrossRef]
76. Song, C.; Wang, T.; Sun, X.; Hu, Y.; Fan, L.; Guo, R. Lubrication performance of MXene/Brij30/H2O composite lamellar liquid crystal system. *Colloids Surf. A Physicochem. Eng. Asp.* **2022**, *641*, 128487. [CrossRef]

77. Chhattal, M.; Rosenkranz, A.; Zaki, S.; Ren, K.; Ghaffar, A.; Gong, Z.; Grützmacher, P.G. Unveiling the Tribological Potential of MXenes-Current Understanding and Future Perspectives. *Adv. Colloid Interface Sci.* **2023**, *321*, 103021. [CrossRef] [PubMed]
78. Marian, M.; Song, G.C.; Wang, B.; Fuenzalida, V.M.; Krauß, S.; Merle, B.; Tremmel, S.; Wartzack, S.; Yu, J.; Rosenkranz, A. Effective usage of 2D MXene nanosheets as solid lubricant-Influence of contact pressure and relative humidity. *Appl. Surf. Sci.* **2020**, *531*, 147311. [CrossRef]
79. Yin, X.; Jin, J.; Chen, X.; Rosenkranz, A.; Luo, J. Ultra-Wear-Resistant MXene-Based Composite Coating via in Situ Formed Nanostructured Tribofilm. *ACS Appl. Mater. Interfaces* **2019**, *11*, 32569–32576. [CrossRef] [PubMed]
80. Zhou, X.; Guo, Y.; Wang, D.; Xu, Q. Nano friction and adhesion properties on Ti_3C_2 and Nb_2C MXene studied by AFM. *Tribol. Int.* **2021**, *153*, 106646. [CrossRef]
81. Das, P.; Ganguly, S.; Rosenkranz, A.; Wang, B.; Yu, J.; Srinivasan, S.; Rajabzadeh, A.R. MXene/0D Nanocomposite Architectures: Design, Properties and Emerging Applications. *Mater. Today Nano* **2023**, *24*, 100428. [CrossRef]
82. Chen, Z.; Zhang, M.; Guo, Z.; Chen, H.; Yan, H.; Ren, F.; Jin, Y.; Sun, Z.; Ren, P. Synergistic effect of novel hyperbranched pol-ysiloxane and Ti_3C_2T MXene/MoS_2 hybrid filler towards desirable mechanical and tribological performance of bismaleimide composites. *Compos. Part B Eng.* **2023**, *248*, 110374. [CrossRef]
83. Guo, L.; Zhang, Y.; Zhang, G.; Wang, Q.; Wang, T. MXene-Al2O3 synergize to reduce friction and wear on epoxy-steel contacts lubricated with ultra-low sulfur diesel. *Tribol. Int.* **2021**, *153*, 106588. [CrossRef]
84. Cui, Y.; Xue, S.; Chen, X.; Bai, W.; Liu, S.; Ye, Q.; Zhou, F. Fabrication of two-dimensional MXene nanosheets loading Cu nano-particles as lubricant additives for friction and wear reduction. *Tribol. Int.* **2022**, *176*, 107934. [CrossRef]
85. Marian, M.; Feile, K.; Rothammer, B.; Bartz, M.; Wartzack, S.; Seynstahl, A.; Tremmel, S.; Krauß, S.; Merle, B.; Böhm, T.; et al. Ti_3C_2T solid lubricant coatings in rolling bearings with remarkable performance beyond state-of-the-art materials. *Appl. Mater. Today* **2021**, *25*, 101202. [CrossRef]
86. Zhou, C.; Li, Z.; Liu, S.; Ma, L.; Zhan, T.; Wang, J. Synthesis of MXene-Based Self-dispersing Additives for Enhanced Tribological Properties. *Tribol. Lett.* **2022**, *70*, 63. [CrossRef]
87. Guo, J.; Wu, P.; Zeng, C.; Wu, W.; Zhao, X.; Liu, G.; Zhou, F.; Liu, W. Fluoropolymer grafted $Ti_3C_2T_x$ MXene as an efficient lubri-cant additive for fluorine-containing lubricating oil. *Tribol. Int.* **2022**, *170*, 107500. [CrossRef]
88. Wang, Q.; Pan, X.; Wang, X.; Cao, S.; Chen, L.; Ma, X.; Huang, L.; Ni, Y. Fabrication strategies and application fields of novel 2D Ti_3C_2Tx (MXene) composite hydrogels: A mini-review. *Ceram. Int.* **2021**, *47*, 4398–4403. [CrossRef]
89. Xue, P.; Bisoyi, H.K.; Chen, Y.; Zeng, H.; Yang, J.; Yang, X.; Lv, P.; Zhang, X.; Priimagi, A.; Wang, L.; et al. Near-Infrared Light-Driven Shape-Morphing of Programmable Anisotropic Hydrogels Enabled by MXene Nanosheets. *Angew. Chem. Int. Ed. Engl.* **2021**, *60*, 3390–3396. [CrossRef]
90. Zhang, P.; Yang, X.J.; Li, P.; Zhao, Y.; Niu, Q.J. Fabrication of novel MXene (Ti_3C_2)/polyacrylamide nanocomposite hydrogels with enhanced mechanical and drug release properties. *Soft Matter* **2020**, *16*, 162–169. [CrossRef]
91. Yan, B.Y.; Cao, Z.K.; Hui, C.; Sun, T.C.; Xu, L.; Ramakrishna, S.; Yang, M.; Long, Y.Z.; Zhang, J. MXene@Hydrogel composite nanofibers with the photo-stimulus response and optical monitoring functions for on-demand drug release. *J. Colloid Interface Sci.* **2023**, *648*, 963–971. [CrossRef] [PubMed]
92. Qin, M.; Yuan, W.; Zhang, X.; Cheng, Y.; Xu, M.; Wei, Y.; Chen, W.; Huang, D. Preparation of PAA/PAM/MXene/TA hydrogel with antioxidant, healable ability as strain sensor. *Colloids Surf. B Biointerfaces* **2022**, *214*, 112482. [CrossRef] [PubMed]
93. Miao, X.; Li, Z.; Hou, K.; Gao, Q.; Huang, Y.; Wang, J.; Yang, S. Bioinspired multi-crosslinking and solid–liquid composite lubricating MXene/PVA hydrogel based on salting out effect. *Chem. Eng. J.* **2023**, *476*, 146848. [CrossRef]
94. Ye, G.; Wen, Z.; Wen, F.; Song, X.; Wang, L.; Li, C.; He, Y.; Prakash, S.; Qiu, X. Mussel-inspired conductive Ti_2C-cryogel promotes functional maturation of cardiomyocytes and enhances repair of myocardial infarction. *Theranostics* **2020**, *10*, 2047–2066. [CrossRef] [PubMed]
95. Quero, F.; Rosenkranz, A. Mechanical Performance of Binary and Ternary Hybrid MXene/Nanocellulose Hydro- and Aerogels—A Critical Review. *Adv Mater. Interfaces* **2021**, *8*, 2100952. [CrossRef]
96. Gogotsi, Y. The Future of MXenes. *Chem. Mater.* **2023**, *35*, 8767–8770. [CrossRef]
97. Naguib, M.; Barsoum, M.W.; Gogotsi, Y. Ten Years of Progress in the Synthesis and Development of MXenes. *Adv. Mater.* **2021**, *33*, 2103393. [CrossRef] [PubMed]
98. Anasori, B.; Gogotsi, Y. MXenes: Trends, Growth, and Future Directions. *Graphene 2D Mater.* **2022**, *7*, 75–79. [CrossRef]
99. Li, K.; Zhao, J.; Zhussupbekova, A.; Shuck, E.C.; Hughes, L.; Dong, Y.; Barwich, S.; Vaesen, S.; Shvets, V.I.; Möbius, M.; et al. 4D printing of MXene hydrogels for high-efficiency pseudocapacitive energy storage. *Nat. Commun.* **2022**, *13*, 6884. [CrossRef]
100. Wyatt, B.; Rosenkranz, A.; Anasori, B. 2D MXenes: Tunable Mechanical and Tribological Properties. *Adv. Mater.* **2021**, *33*, 2007973. [CrossRef]
101. Rosenkranz, A.; Righi, M.; Sumant, A.; Anasori, B.; Mochalin, V. Perspectives of 2D MXene Tribology. *Adv. Mater.* **2023**, *35*, 2207757. [CrossRef] [PubMed]
102. Parra-Munoz, N.; Soler, M.; Rosenkranz, A. Covalent functionalization of MXenes for tribological purposes—A critical review. *Adv. Colloid Interface Sci.* **2022**, *309*, 102792. [CrossRef] [PubMed]
103. Chakrabarty, A.; Maitra, U.; Das, A. Metal cholate hydrogels: Versatile supramolecular systems for nanoparticle embedded soft hybrid materials. *J. Mater. Chem.* **2012**, *22*, 18268. [CrossRef]

104. Chen, L.; He, C.; Yin, J.; Chen, S.; Zhao, W.; Zhao, C. Clearance of methylene blue by CdS enhanced composite hydrogel materials. *Environ. Technol.* **2020**, *43*, 355–366. [CrossRef] [PubMed]
105. Wei, L.; Li, Z.; Li, J.; Zhang, Y.; Yao, B.; Liu, Y.; Song, W.; Fu, X.; Wu, X.; Huang, S. An approach for mechanical property optimiza-tion of cell-laden alginate–gelatin composite bioink with bioactive glass nanoparticles. *J. Mater. Sci. Mater. Med.* **2020**, *31*, 103. [CrossRef]
106. Dai, C.; Zhang, X.; Du, C.; Frank, A.; Schmidt, H.; Zheng, Q.; Wu, Z. Photoregulated Gradient Structure and Programmable Me-chanical Performances of Tough Hydrogels with a Hydrogen-Bond Network. *ACS Appl. Mater. Interfaces* **2020**, *12*, 53376–53384. [CrossRef]
107. Wang, Z.; Yang, H.; Liang, H.; Xu, Y.; Zhou, J.; Peng, H.; Zhong, J.; Xi, W. Polydopamine particles reinforced poly(vinyl alcohol) hydrogel composites with fast self healing behavior. *Prog. Org. Coat.* **2020**, *143*, 105636. [CrossRef]
108. Du, Z.; Wang, Y.; Li, X. Preparation of Nanocellulose Whisker/Polyacrylamide/Xanthan Gum Double Network Conductive Hydrogels. *Coatings* **2023**, *13*, 843. [CrossRef]
109. Yang, B.; Zhang, S.; Wang, P.; Liu, C.; Zhu, Y. Robust and rapid responsive organic-inorganic hybrid bilayer hydrogel actuators with silicon nanoparticles as the cross-linker. *Polymer* **2021**, *228*, 123863. [CrossRef]
110. Li, S.; Wang, X.; Zhu, J.; Wang, Z.; Wang, L. Synthesis and characterization of photothermal antibacterial hydrogel with enhanced mechanical properties. *New J. Chem.* **2021**, *45*, 16804–16815. [CrossRef]
111. Lu, Y.; Han, J.; Ding, Q.; Yue, Y.; Xia, C.; Ge, S.; Le, Q.; Dou, X.; Sonne, C.; Lam, S. TEMPO-oxidized cellulose nanofibers/polyacrylamide hybrid hydrogel with intrinsic self-recovery and shape memory properties. *Cellulose* **2021**, *28*, 1469–1488. [CrossRef]
112. Abalymov, A.; Lengert, E.; Van der Meeren, L.; Saveleva, M.; Ivanova, A.; Douglas, T.; Skirtach, A.; Volodkin, D.; Parakhonskiy, B. The influence of Ca/Mg ratio on autogelation of hydrogel biomaterials with bioceramic compounds. *Biomater. Adv.* **2022**, *133*, 112632. [CrossRef] [PubMed]
113. Xiao, H.; Liu, S. 2D nanomaterials as lubricant additive: A review. *Mater. Des.* **2017**, *135*, 319–332. [CrossRef]
114. Liu, Y.; Yu, S.; Fan, Z.; Ge, X.; Wang, W. How does lateral size influence the tribological behaviors of graphene oxide as nanoadditive for water-based lubrication? *Carbon* **2024**, *219*, 118803. [CrossRef]
115. Zhang, N.; Hong, Y.; Yazdanparast, S.; Asle, M. Superior structural, elastic and electronic properties of 2D titanium nitride MXenes over carbide MXenes: A comprehensive first principles study. *2D Mater.* **2018**, *5*, 45004. [CrossRef]
116. Kurtoglu, M.; Naguib, M.; Gogotsi, Y.; Barsoum, M. First principles study of two-dimensional early transition metal car-bides. *MRS Commun.* **2012**, *2*, 133–137. [CrossRef]
117. Ronchi, R.; Lemos, H.; Nishihora, R.; Cuppari, M.; Santos, S. Tribology of polymer-based nanocomposites reinforced with 2D materials. *Mater. Today Commun.* **2023**, *34*, 105397. [CrossRef]
118. Lang, J.; Ding, B.; Zhang, S.; Su, H.; Ge, B.; Qi, L.; Gao, H.; Li, X.; Li, Q.; Wu, H. Scalable Synthesis of 2D Si Nanosheets. *Adv. Mater.* **2017**, *29*, 1701777. [CrossRef]
119. Liu, Y.; Yu, S.; Wang, W. Nanodiamond plates as macroscale solid lubricant: A "non-layered" two-dimension material. *Carbon* **2022**, *198*, 119–131. [CrossRef]
120. Liu, Y.; Yu, S.; Zhang, R.; Ge, X.; Wang, W. "Non-layered" two-dimensional nanodiamond plates as nanoadditives in water lubrication. *Wear* **2024**, *536–537*, 205174. [CrossRef]
121. Serles, P.; Arif, T.; Puthirath, A.; Yadav, S.; Wang, G.; Cui, T.; Balan, A.; Yadav, T.; Thibeorchews, P.; Chakingal, N.; et al. Friction of magnetene, a non–van der Waals 2D material. *Sci. Adv.* **2021**, *7*, 2041. [CrossRef] [PubMed]